Journal of Magnetic Resonance 200 (2009) 137–141

Contents lists available at ScienceDirect

Journal of Magnetic Resonance

journal homepage: www.elsevier.com/locate/jmr

Communication

Overhauser dynamic nuclear polarization and molecular dynamics simulations using pyrroline and piperidine ring nitroxide radicals

Brandon D. Armstrong [a], Patricia Soto [b,1], Joan-Emma Shea [a,b], Songi Han [b,*]

[a] Department of Physics, University of California, Santa Barbara, CA 93106, USA
[b] Department of Chemistry and Biochemistry, University of California, Santa Barbara, CA 93106, USA

ARTICLE INFO

Article history:
Received 28 March 2009
Revised 25 May 2009
Available online 2 June 2009

Keywords:
Dynamic nuclear polarization
Overhauser effect
Nitroxide radicals
Molecular dynamics simulations
Field cycling relaxometry
Nuclear magnetic resonance dispersion

ABSTRACT

The efficiency of Overhauser dynamic nuclear polarization (DNP) depends on the local dynamics modulating the dipolar coupling between the two interacting spins. By attaching nitroxide based spin labels to molecules and by measuring the ^{1}H DNP response of solvent water, information about the local hydration dynamics near the spin label can be obtained. However, there are two commonly used types of nitroxide ring structures; a pyrroline based and a piperidine based molecule. It is important to know when comparing different experiments, whether changes in DNP enhancements are due to changes in local hydration dynamics or because of the different spin label structures. In this study we investigate the key parameters affecting DNP signal enhancements for 3-carbamoyl-2,2,5,5-tetramethyl-3-pyrrolin-1-oxyl, a 5-membered ring nitroxide radical, and for 4-oxo-2,2,6,6-tetramethyl-1-piperidinyloxy, a 6-membered ring nitroxide radical. Using X-Band DNP, field cycling relaxometry, and molecular dynamics simulations, we conclude that the key parameters affecting the DNP amplitude of the ^{1}H signal of water to be equal when using either nitroxide. Thus, experiments measuring hydration dynamics using either type of spin labels may be compared.

1. Introduction

The structure and function of many biological molecules and assemblies are mediated by local hydration dynamics at their surface and interfaces. The ability to measure these hydration dynamics is important to characterizing protein folding or understanding water transport across lipid membranes [1–4]. However, as surface water does not provide a unique spectroscopic signature distinct from bulk water, experimental measurements of local hydration dynamics are difficult. Overhauser dynamic nuclear polarization (DNP) makes use of the dipolar coupling between an unpaired electron and solvent nuclei (the unpaired electron of a nitroxide radical and the ^{1}H of water in this report) to hyperpolarize the nuclear magnetic resonance (NMR) signal. The NMR signal enhancement (E) is sensitive to the local dynamics modulating the dipolar coupling between the two spins through its dependence on the coupling factor, ρ, as described in Eq. (1) [5,6].

$$E = 1 - \rho(\tau) f s \frac{|\gamma_S|}{\gamma_I}. \quad (1)$$

The leakage factor, f, describes how efficiently the electron spin relaxes the nuclear spin. The saturation factor, s, gives the degree of electron spin saturation by means of microwave irradiation and hyperfine mixing of the electron spin transitions [7,8]. The coupling factor contains the dynamic information of the interacting, spin-bearing molecules through its dependence on the translational correlation time, τ, shown in Eq. (2). Here, d is the distance of closest approach between the unpaired electron and the nuclei to be polarized, and D_I and D_S are the diffusion coefficients of the nuclear and electron spin-bearing molecules, respectively [5].

$$\tau = \frac{d^2}{D_I + D_S}. \quad (2)$$

By making use of the common nitroxide spin probes attached to a biological molecule, and by measuring the corresponding ^{1}H signal enhancement of the solvent water, information on the local solvent dynamics near the spin probe can be obtained [6]. There are two widely used types of nitroxide radicals; a pyrroline (5-membered ring) based and a piperidine (6-membered ring) based ring structure. The 5-ring nitroxide is almost exclusively used to spin label proteins, while the 6-ring nitroxide is often used to label lipid head groups and it is a common polarizing agent for DNP experiments. As the correlation time given in Eq. (2) depends on d^2, it is important to know whether the two different nitroxide molecules approach the water protons with the same distance of closest

* Corresponding author.
E-mail address: songi@chem.ucsb.edu (S. Han).
[1] Present address: Department of Physics, Creighton University, Omaha, NE 68178, USA.

1090-7807/$ - see front matter © 2009 Elsevier Inc. All rights reserved.
doi:10.1016/j.jmr.2009.05.013

approach. It is also important to know if the coordination number (number of protons hydrogen bonded to the oxygen on the nitroxide) and hydrogen bond lifetimes are similar, and whether they are necessary parameters to include for extracting hydration dynamics from DNP experiments. Significant hydrogen bonding between the nitroxide radicals and water would require the inclusion of a rotational correlation time in addition to the translational correlation time shown in Eq. (2) [5]. The two correlation times are not easily separated without making measurements at different magnetic fields.

An earlier study comparing many different 5-ring and 6-ring based nitroxide radicals found a wide range of coupling factors [9]. However, this study neglected the effect of Heisenberg spin exchange which is known to have a large effect on the saturation factor, *s*, and thus on the measured and maximum DNP enhancement factor [6–8]. Our own experiments do not confirm the large dependence on the nitroxide's functional group observed in Ref. [9]. This discrepancy is likely due to ignoring Heisenberg spin exchange in their analysis [10].

In a previous study, DNP and FCR measurements of the 6-ring nitroxide 4-oxo-2,2,6,6-tetramethyl-1-piperidinyloxy (tempo) were performed [6]. Here, we compare those results to DNP and FCR experiments carried out on the 5-ring nitroxide 3-carbamoyl-2,2,5,5-tetramethyl-3-pyrrolin-1-oxyl (proxyl) (Fig. 1). Additionally, molecular dynamics (MD) simulations have been carried out for both the 5-ring and 6-ring nitroxide radicals, and the hydration dynamics of each radical compared, with the focus on determining if there are differences in the properties relevant for their DNP performance.

2. Results and discussion

2.1. X-band DNP

DNP experiments were performed using a homebuilt, high power microwave source described previously [10]. Each radical was dissolved in water, and 4–5 μL of this sample was loaded into a silica capillary, sealed with beeswax, and placed in a homebuilt 14.85 MHz NMR probe. The ^{1}H NMR signal enhancement for each sample was measured as a function of applied microwave power. The results were extrapolated to infinite power to determine the maximum signal enhancement, E_{max}. In the limit of infinite radical

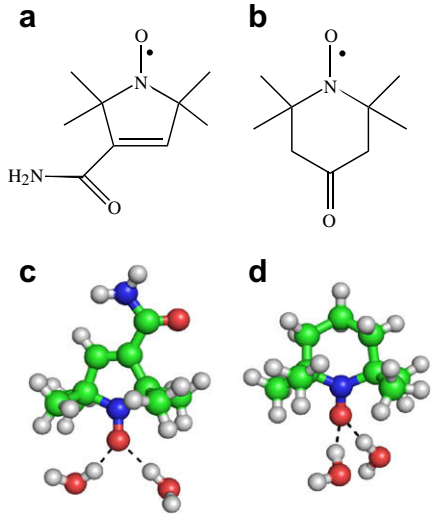

Fig. 1. Chemical structure of (a) proxyl and (b) tempo purchased from Sigma–Aldrich and used for DNP and FCR experiments. Using PyMOL (Ref. [18]); the structure of (c) proxyl and (d) tempo used in MD simulations with an example of the orientation of hydrogen bonded water molecules.

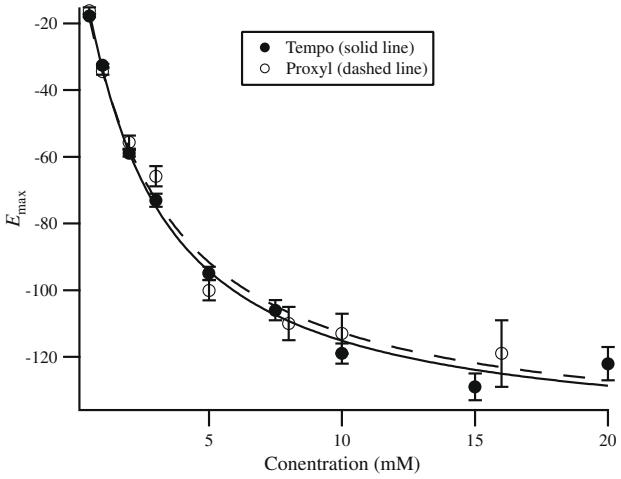

Fig. 2. E_{max} versus concentration for both tempo and proxyl radicals and the fit of the data taking into account the concentration dependence of both the leakage and saturation factors (see Ref. [6]). For both molecules, the E_{max} values give a coupling factor of 0.22. NMR data were taken at 0.35 T using a Bruker Avance 300 spectrometer. A Bruker TE_{102} resonant cavity was used for microwave irradiation. See Ref. [10] for more experimental details.

concentration, both *f* and *s* approach 1 and $E_{max} \to 1 - 658\rho$ [6,7]. Fig. 2 shows the measured E_{max} values for a series of concentrations for both tempo and proxyl radicals. The fit curves take the concentration dependence of both the leakage and saturation factors into account as detailed in Ref. [6]. For each concentration, both radicals give the same NMR signal enhancement within error, and the measured coupling factor for each radical was determined to be 0.22 ± 0.01. Equal DNP efficiency for water implies that the translational correlation time between the spin label and water is equal for both the 5-ring and 6-ring species, provided a pure translational model for the nitroxide-water system is a good approximation. This assumption is supported by our FCR and MD results discussed below.

As discussed in a different report, a coupling factor of 0.22 implies τ = 76 ps [6]. Using DOSY, the measured self diffusion coefficient of tempo in solution was found to be 4.1×10^{-10} m^2 s^{-1}. Putting this value into Eq. (2) along with the self diffusion coefficient of water (2.3×10^{-9} m^2 s^{-1} [11]) gives *d* = 4.5 Å for hydrated spin label environments. The assumption that the self diffusion of bulk water can be used as the D_I value for water directly interacting with the nitroxide radical is supported by our MD studies discussed below and by previous FCR experiments between nitroxide radicals and small charged solutes [12].

2.2. Field cycling relaxometry

Field cycling relaxometry is a technique related to DNP as it also takes advantage of the increased ^{1}H relaxation of the solvent due to the presence of paramagnetic species. Both phenomena are mediated through the translational diffusion of water with respect to free nitroxide radicals for effective dipolar cross relaxation between ^{1}H and electron spins. Measuring the ^{1}H relaxation rate at many different magnetic fields gives insight into the shape of the spectral density function describing the dynamics between the two spins. The hard sphere, force free, model has been previously applied to nitroxide radicals, giving a good fit to the data. In this case the T_1 relaxation rate of the ^{1}H of water is given by [13]

$$\frac{1}{T_1} = \frac{1}{T_{10}(\omega)} + \frac{32\pi}{405}\gamma_I^2\gamma_S^2\hbar^2 S(S+1) \frac{N_A}{1000} C \frac{\tau}{d^3}\left(6J(\omega_S+\omega_I,\tau) + 3J(\omega_I,\tau) + J(\omega_S-\omega_I,\tau)\right) \quad (3)$$

where S is the spin of the electron (1/2), C is the radical concentration, N_A is Avagadro's number, T_{10} is the relaxation rate of ^{1}H in the absence of the unpaired electron, and the spectral density function is given by [13–15]

$$J(\omega,\tau)=\frac{1+\frac{5\sqrt{2}}{8}(\omega\tau)^{1/2}+\frac{\omega\tau}{4}}{1+(2\omega\tau)^{1/2}+(\omega\tau)+\frac{\sqrt{2}}{3}(\omega\tau)^{3/2}+\frac{16}{81}(\omega\tau)^{2}+\frac{4\sqrt{2}}{81}(\omega\tau)^{5/2}+\frac{(\omega\tau)^{3}}{81}}. \quad (4)$$

The distance of closest approach and translational correlation time are the fit parameters in an FCR experiment making use of this model.

Fig. 3 shows the results of the field cycling data for both tempo and proxyl radicals at 5 mM spin label concentration. The fit of the data to Eq. (3) for tempo gives d = 2.43 Å and τ = 24 ps while that for proxyl gives d = 2.36 Å and τ = 27 ps. These results are remarkably close to each other, and provide further evidence that the dipolar coupling between the unpaired electron and ^{1}H of water is not affected by the properties of the 6-ring versus 5-ring structure, and that the key DNP parameters are the same for each radical. In agreement with previous FCR studies using nitroxide radicals [12,13,16,17], the translational model fits the data well; supporting the approximation that complex formation and rotational effects can be ignored in our DNP analysis. Our MD studies discussed below provide further support for this approximation.

Fig. 3 appears to show that proxyl relaxes the ^{1}H of water more efficiently than tempo, even though for each radical concentration proxyl and tempo give nearly equal DNP enhancements as shown in Fig. 2. Since Eq. (3) depends on $1/d^3$, FCR may be more sensitive to very small changes in the distance of closest approach, such as 2.43 versus 2.36 Å, which are negligible differences in the context of examining hydration dynamics in the local vicinity of spin labels. Another likely explanation is that the two solutions contained slightly different radical concentrations since Eq. (3) also depends on the sample concentration. So, even if the d for each radical was assumed to be equal, only a change in C of <10% is necessary to bring the two curves together.

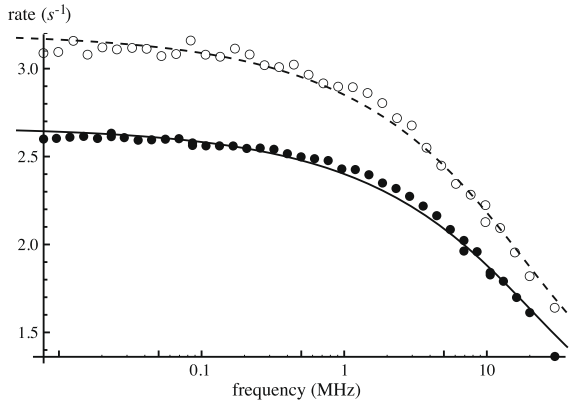

Fig. 3. Field cycling data for both 5 mM tempo and 5 mM proxyl taken at the Technical University of Illmenau on a Stelar FFC 2000-1T Field Cycling Relaxometer. The solid and dashed curves are the fit of the data to Eq. (3).

The discrepancy of the absolute values for d and τ from FCR versus DNP (discussed in detail in Ref. [6]) is likely due to shortcomings of the currently available spectral density function with the approximation of treating the molecules as hard spheres with no forces acting between them. Polnaszek and Bryant examined the effects of removing the spin centered, hard sphere assumptions on the spectral density function and found that for nitroxides in solution there was little change in the shape of the curve or fit parameters [16]. The discrepancy between the DNP and FCR analysis remains unresolved [6,17]. It is important to note that ρ obtained from the DNP analysis is independent of the employed dynamic model underlying the spectral density function. The key finding here is that the 5-ring and 6-ring nitroxide radicals behave identically in the context of DNP and FCR experiments, which rely on the dipolar coupling between the electron and ^{1}H nuclear spin. Therefore, DNP experiments making use of either structure may be compared, and changes in E_{max} can be interpreted as changes in the dynamics modulating the dipolar coupling, and not due to changes in the structure of the radical.

2.3. Molecular dynamics simulations

Extensive MD simulations were carried out on the 5-ring and 6-ring structures shown in Fig. 1c and d [18] to further elucidate the conclusions from our DNP and FCR analysis. Pavone et al. have previously performed Car-Parrinello MD simulations on proxyl for the interpretation and simulation of ESR spectra [19,20]. In our search of the literature, however, we did not find a comparison of the parameters relevant to the expected DNP efficiency between proxyl and tempo. Details of the simulation are described at the end of this report.

Table 1 summarizes the results of our simulations. The results of proxyl are in excellent agreement with those of Pavone and colleagues [19,20]. While there are small differences in the results depending on the water model used (a 3-site SPC-E model and a 4-site TIP4P model), there is good agreement in the values between proxyl and tempo. On average, two hydrogen nuclei (one from two different water molecules) are hydrogen bound to the nitroxide radical, but this lifetime is very short (4–6 ps) compared to the 26 ps rotational tumbling time of a tempo molecule as experimentally found by Robinson et al. [21] so rotational diffusion is not expected to contribute much to the ^{1}H nuclear spin relaxation rate. In light of this evidence of hydrogen bonding, we applied a mixed rotation and translation diffusion model to fit the FCR data. By adding a 9% rotational component we were able to improve the fit, but at the cost of three additional fit parameters to the model. Additionally, the fit values for d and τ changed by less than 5%. Thus both MD simulations and the FCR data justify our use of a pure translational model as a good approximation to the system. This is an important finding for extracting hydration dynamic information from a ^{1}H DNP experiment. If a mixed phase model is required,

Table 1
Comparison of proxyl and tempo MD results. For each radical, the distance between the center of mass (com) of the N–O bond and ^{1}H of water, the number of hydrogen bonded water protons, and the lifetime of hydrogen bonds is nearly identical. Reported distances represent the first peak of the radial distribution function. The diffusion of water around the radical is identical to bulk within the error of the simulations. Simulated bulk water diffusion coefficients were taken from Ref. [22].

		NO_{com}–$H_{solvent}$ (Å)	Coordination	H-bond lifetime (ps)	D_l (near radical) ($m^2\ s^{-1}$)	D_l (bulk) ($m^2\ s^{-1}$)
Proxyl	TIP4P	2.3	2.0 ± 0.7	4.6 ± 0.2	$(4.1 \pm 0.4) \times 10^{-9}$	4.0×10^{-9}
	SPC/E	2.2	2.0 ± 0.7	5.5 ± 0.4	$(3.0 \pm 0.3) \times 10^{-9}$	2.9×10^{-9}
Tempo	TIP4P	2.3	1.7 ± 0.7	4.3 ± 0.2	$(4.3 \pm 0.4) \times 10^{-9}$	4.0×10^{-9}
	Spc/E	2.2	1.9 ± 0.6	5.0 ± 0.3	$(3.1 \pm .03) \times 10^{-9}$	2.9×10^{-9}

it is not possible to extract a single correlation time from a DNP experiment at a single magnetic field.

A DNP experiment cannot report directly on d, but only on τ. Therefore, measurements of the diffusion coefficients of both the solvent and the solute are necessary if d is to be determined. However, as the dipolar coupling is a local effect with 90% of the relaxation occurring within 10 Å [16], a bulk solvent diffusion measurement may not accurately reflect the diffusion of the solvent near the radical, leading to an erroneous τ. Our simulations, however, clearly show that the self diffusion coefficient of water directly interacting with the radical is in agreement with the simulated values for the self diffusion coefficient of bulk water reported in the literature [22]. Note that the absolute value for water diffusion coefficients from MD simulations differs from the experimental value (2.3×10^{-9} m^2 s^{-1}), but this is a known and accepted discrepancy of the water models used in the simulations. The finding that the spin label does not alter the diffusion dynamics of nearby water molecules justifies our use of $\sim 2.3 \times 10^{-9}$ m^2 s^{-1} for D_I in Eq. (2), and further supports the feasibility of measuring local hydration dynamics through DNP analysis via spin labels. In bulk water, the local hydration dynamics measured through free spin labels correspond to the self diffusion coefficient of bulk water without spin labels, as it should. When the spin label is tethered to a larger molecule, the spin label will probe the altered hydration dynamics of water interacting with the larger molecule's surface in the vicinity (<10 Å) of the tethered spin label.

3. Conclusion

Taking advantage of two different magnetic resonance experimental techniques and molecular dynamics simulations, we have observed no difference in any of the key DNP parameters which would affect the coupling factor between water and the six ring nitroxide 4-oxo-2,2,6,6-tetramethyl-1-piperidinyloxy or the five ring nitroxide 3-carbamoyl-2,2,5,5-tetramethyl-3-pyrrolin-1-oxyl spin probes. There were some discrepancies between the absolute values obtained from each technique, but there is clear agreement between the parameters obtained for the 5 versus 6-ring nitroxide probes. Our study shows that the differences in the 5 versus 6-ring nitroxide structures do not alter the local order or dynamics of water that is interacting with these spin labels. This implies that when comparing experiments making use of 5-ring and 6-ring nitroxide radicals as spin labels on biomolecules, changes in the DNP coupling factor can be associated with changes in local solvent dynamics around the spin labels and not the different ring structures. It is important to point out that actual measured enhancements may be quite different when using different radicals as the ESR linewidth of radicals with different structures and different functional groups was found to vary. However, changes in enhancements due to ESR linewidth do not affect the measurement of ρ, which is found by measuring E_{max} for many concentrations and by extrapolating to infinite concentration [7]. We have also ignored possible changes in T_1 and T_2 of the electron spins that are observed and expected due to the different molecular structures. For our purpose, this is a valid assumption because for nitroxide radicals both T_{1e} and $T_{2e} >> \tau$, and thus can be ignored in the spectral density function [13,14]. So, a nitroxide spin label can be chosen based on symmetry or ease of chemical modification. This is not the case in electron spin resonance studies where the spectrum is highly dependent on the dynamics of the electron spin probe itself, which changes significantly depending on the tethering chemistry to the macromolecule. Overhauser DNP, on the other hand, is dominated by the much faster motion of the local solvent around the spin labels, making it a viable tool to quantify local hydration dynamics through the use of site specific spin labeling.

4. MD simulation methods

Classical MD simulations were performed using the GROMACS.x software package [22,23]. The all-atom OPLS force field [24,25] was used to describe the solute while two different models, TIP4P [26] and SPC/E [27], were used to describe the solvent. Temperature and pressure were maintained close to 300 K and 1 bar by weak coupling to an external bath [28] with a coupling constant of 0.1 ps for temperature and 1.0 ps for pressure. The LINCS [29] algorithm was used to constrain bond lengths within the solute. The SETTLE [30] algorithm was used to constrain bond lengths and the bond angle in water. The integration time step was 2 fs. A smooth particle mesh Ewald method [31] was used to evaluate Coulomb interactions with a real-space cut-off of 0.9 nm, grid spacing of 0.12, and quadratic interpolation. van der Waals interactions were evaluated using a cut-off method, with a cut-off distance of 0.9 nm. Neighbors lists were updated every five steps. The structure of each solute was initially generated with Molden [32] and then optimized at the level of HF/6-13G$*$ using Gaussian 03 [33]. Partial charges on the atoms were obtained by fitting the gas phase electrostatic potential calculated at the HF/6-13G$*$ level using RESP [34]. The solute molecule was initially solvated in a periodic 21.45 nm^3 box. Initial velocities were assigned from a Maxwellian distribution at 300 K. Cartesian coordinates were stored every 100 fs. For data acquisition in each solvent model, an initial 2 ns trajectory was generated. Then ten snapshots from this trajectory were chosen to initiate 10 independent 2 ns trajectories, of which the first 200 ps was disregarded for analysis. Values are reported after averaging over the 10 independent trajectories.

Acknowledgments

We thank Prof. Siegfried Stapf and Dr. Carlos Mattea at the Technical University of Illmenau for performing the field cycling relaxometry measurements reported here. We thank Evan McCarney for helpful discussions. Computer support was provided by the Lonestar cluster at the Texas Advanced Computing Center (LRAC MCA 05S027). This work was partially supported by the MRL program of the National Science Foundation under Grant No. DMR05-20415, the Faculty Early Career Award (Grant CHE-0645536), the W.M. Keck Award for Science and Engineering, the David and Lucile Packard Foundation, and NSF Grant MCB 0642086.

References

[1] P. Liu, X.H. Huang, R.H. Zhou, B.J. Berne, Observation of a dewetting transition in the collapse of the melittin tetramer, Nature 437 (2005) 159–162.
[2] S. Nishiguchi, Y. Goto, S. Takahashi, Solvation and desolvation dynamics in apomyoglobin folding monitored by time-resolved infrared spectroscopy, J. Mol. Biol. 373 (2007) 491–502.
[3] K. Wood, M. Plazanet, F. Gabel, B. Kessler, D. Oesterhelt, D.J. Tobias, G. Zaccai, M. Weik, Coupling of protein and hydration-water dynamics in biological membranes, Proc. Natl. Acad. Sci. USA 104 (2007) 18049–18054.
[4] F. Xu, T.A. Cross, Water: foldase activity in catalyzing polypeptide conformational rearrangements, Proc. Natl. Acad. Sci. USA 96 (1999) 9057–9061.
[5] K.H. Hausser, D. Stehlik, Dynamic nuclear polarization in liquids, Adv. Magn. Reson. 3 (1968) 79–139.
[6] B.D. Armstrong, S. Han, Overhauser dynamic nuclear polarization to study local water dynamics, J. Am. Chem. Soc. 131 (2009) 4641–4647.
[7] B.D. Armstrong, S. Han, A new model for Overhauser enhanced nuclear magnetic resonance using nitroxide radicals, J. Chem. Phys. 127 (2007) 104508–104510.
[8] R.D. Bates, W.S. Drozdoski, Use of nitroxide spin labels in studies of solvent–solute interactions, J. Chem. Phys. 67 (1977) 4038–4044.
[9] D. Grucker, T. Guiberteau, B. Eclancher, J. Chambron, R. Chiarelli, A. Rassat, G. Subra, B. Gallez, Dynamic nuclear-polarization with nitroxides dissolved in biological-fluids, J. Magn. Reson. B 106 (1995) 101–109.
[10] B.D. Armstrong, M.D. Lingwood, E.R. McCarney, E.R. Brown, P. Blümler, S. Han, Portable X-band system for solution state dynamic nuclear polarization, J. Magn. Reson. 191 (2008) 273–281.

[11] K.-H. Herrmann, A. Pohlmeier, D. Gembris, H. Vereecken, Three-dimensional imaging of pore water diffusion and motion in porous media by nuclear magnetic resonance imaging, J. Hydrol. 267 (2002) 244–257.
[12] T.R.J. Dinesen, J. Seymour, L. McGowan, S. Wagner, R.G. Bryant, ^{19}F and ^{1}H magnetic resonance relaxation dispersion determination of the translational encounter between ionic salts and nitroxide free radicals in aqueous solution, J. Phys. Chem. A 103 (1999) 782–786.
[13] M.W. Hodges, D.S. Cafiso, C.F. Polnaszek, C.C. Lester, R.G. Bryant, Water translational motion at the bilayer interface: an NMR relaxation dispersion measurement, Biophys. J. 73 (1997) 2575–2579.
[14] J.H. Freed, Dynamic effects of pair correlation functions on spin relaxation by translational diffusion in liquids. II. Finite jumps and independent T_1 processes, J. Chem. Phys. 68 (1978) 4034–4037.
[15] L.-P. Hwang, J.H. Freed, Dynamic effects of pair correlation functions on spin relaxation by translational diffusion in liquids, J. Chem. Phys. 63 (1975) 4017–4025.
[16] C.F. Polnaszek, R.G. Bryant, Nitroxide radical induced solvent proton relaxation: measurement of localized translational diffusion, J. Chem. Phys. 81 (1984) 4038–4045.
[17] P. Höfer, G. Parigi, C. Luchinat, P. Carl, G. Guthausen, M. Reese, T. Carlomagno, C. Griesinger, M. Bennati, Field dependent dynamic nuclear polarization with radicals in aqueous solution, J. Am. Chem. Soc. 130 (2008) 3254–3255.
[18] W.L. DeLano, The PyMOL Molecular Graphics System, DeLano Scientific LLC, Palo Alto, CA, 2008.
[19] M. Pavone, P. Cimino, O. Crescenzi, A. Sillanpaa, V. Barone, Interplay of intrinsic, environmental, and dynamic effects in tuning the EPR parameters of nitroxides: further insights from an integrated computational approach, J. Phys. Chem. B 111 (2007) 8928–8939.
[20] M. Pavone, A. Sillanpaa, P. Cimino, O. Crescenzi, V. Barone, Evidence of variable H-bond network for nitroxide radicals in protic solvents, J. Phys. Chem. B 110 (2006) 16189–16192.
[21] B.H. Robinson, D.A. Haas, C. Mailer, Molecular-dynamics in liquids—spin–lattice relaxation of nitroxide spin labels, Science 263 (1994) 490–493.
[22] D. van der Spoel, P.J. van Maaren, H.J.C. Berendsen, A systematic study of water models for molecular simulation: derivation of water models optimized for use with a reaction field, J. Chem. Phys. 108 (1998) 10220–10230.
[23] H.J.C. Berendsen, D. van der Spoel, R. van Drunen, GROMACS: a message-passing parallel molecular dynamics implementation, Comput. Phys. Commun. 91 (1995) 43–56.
[24] W.L. Jorgensen, J. Tirado-Rives, The OPLS [optimized potentials for liquid simulations] potential functions for proteins, energy minimizations for crystals of cyclic peptides and crambin, J. Am. Chem. Soc. 110 (1988) 1657–1666.
[25] G.A. Kaminski, R.A. Friesner, J. Tirado-Rives, W.L. Jorgensen, Evaluation and reparametrization of the OPLS-AA force field for proteins via comparison with accurate quantum chemical calculations on peptides, J. Phys. Chem. B 105 (2001) 6474–6487.
[26] W.L. Jorgensen, J. Chandrasekhar, J.D. Madura, R.W. Impey, M.L. Klein, Comparison of simple potential functions for simulating liquid water, J. Chem. Phys. 79 (1983) 926–935.
[27] H.J.C. Berendsen, J.R. Grigera, T.P. Straatsma, The missing term in effective pair potentials, J. Phys. Chem. 91 (1987) 6269–6271.
[28] H.J.C. Berendsen, J.P.M. Postma, W.F. van Gunsteren, A. DiNola, J.R. Haak, Molecular dynamics with coupling to an external bath, J. Chem. Phys. 81 (1984) 3684–3690.
[29] B. Hess, H. Bekker, H.J.C. Berendsen, J.G.E.M. Fraaije, LINCS: a linear constraint solver for molecular simulations, J. Comput. Chem. 18 (1997) 1463–1472.
[30] S. Miyamoto, P.A. Kollman, Settle: an analytical version of the SHAKE and RATTLE algorithm for rigid water models, J. Comput. Chem. 13 (1992) 952–962.
[31] U. Essmann, L. Perera, M.L. Berkowitz, T. Darden, H. Lee, L.G. Pedersen, A smooth particle mesh Ewald method, J. Chem. Phys. 103 (1995) 8577–8593.
[32] G. Schaftenaar, J.H. Noordik, Molden: a pre- and post-processing program for molecular and electronic structures, J. Comput. Aid. Mol. Des. 14 (2000) 123–134.
[33] M.J. Frisch et al., Gaussian 03, Revision D.02, Gaussian Inc., Wallingford, CT, 2004.
[34] C.I. Bayly, P. Cieplak, W. Cornell, P.A. Kollman, A well-behaved electrostatic potential based method using charge restraints for deriving atomic charges: the RESP model, J. Phys. Chem. 97 (1993) 10269–10280.